Journal of Cerebral Blood Flow & Metabolism (2012) 32, 2023–2032

www.jcbfm.com

MRI measurement of angiogenesis and the therapeutic effect of acute marrow stromal cell administration on traumatic brain injury

Lian Li[1], Michael Chopp[1,2], Guang Liang Ding[1], Chang Sheng Qu[3], Qing Jiang Li[1], Mei Lu[4], Shiyang Wang[2], Siamak P Nejad-Davarani[1], Asim Mahmood[3] and Quan Jiang[1,2]

[1]*Department of Neurology, Henry Ford Hospital, Detroit, Michigan, USA;* [2]*Department of Physics, Oakland University, Rochester, Michigan, USA;* [3]*Department of Neurosurgery, Henry Ford Hospital, Detroit, Michigan, USA;* [4]*Department of Biostatistics and Research Epidemiology, Henry Ford Hospital, Detroit, Michigan, USA*

Using magnetic resonance imaging (MRI), the present study was undertaken to investigate the therapeutic effect of acute administration of human bone marrow stromal cells (hMSCs) on traumatic brain injury (TBI) and to measure the temporal profile of angiogenesis after the injury with or without cell intervention. Male Wistar rats (300 to 350 g, $n=18$) subjected to controlled cortical impact TBI were intravenously injected with 1 mL of saline ($n=9$) or hMSCs in suspension ($n=9$, 3×10^6 hMSCs) 6 hours after TBI. *In-vivo* MRI acquisitions of T2-weighted imaging, cerebral blood flow (CBF), three-dimensional (3D) gradient echo imaging, and blood-to-brain transfer constant (Ki) of contrast agent were performed on all animals 2 days after injury and weekly for 6 weeks. Sensorimotor function and spatial learning were evaluated. Volumetric changes in the trauma-induced brain lesion and the lateral ventricles were tracked and quantified using T2 maps, and hemodynamic alteration and blood–brain barrier permeability were monitored by CBF and Ki, respectively. Our data show that transplantation of hMSCs 6 hours after TBI leads to reduced cerebral atrophy, early and enhanced cerebral tissue perfusion and improved functional outcome compared with controls. The hMSC treatment increases angiogenesis in the injured brain, which may promote neurologic recovery after TBI.
Journal of Cerebral Blood Flow & Metabolism (2012) **32,** 2023–2032; doi:10.1038/jcbfm.2012.106; published online 11 July 2012

Keywords: angiogenesis; marrow stromal cells; MRI; perfusion; ventricular dilation

Introduction

Rather than a simple impact event, traumatic brain injury (TBI) is the beginning of an ongoing, perhaps lifelong disease process that causes widespread brain damage regardless of the location of the primary injury, and may lead to chronic disability with lasting cognitive and motor disorders (Masel and DeWitt, 2010). Unfortunately, there is no clinical treatment available to effectively interrupt this secondary injury process (Parr *et al*, 2007), and neuroprotective clinical trials for TBI have shown no benefits (Xiong *et al*, 2009*a*).

Cell transplantation has potential as an effective therapeutic strategy to attenuate secondary injury after TBI that diffusely affects brain (Chopp and Li, 2006; Opydo-Chanek, 2007). Therapeutic benefits of cell-based therapy for brain injury include reconstitution of the blood–brain barrier (BBB), restoration of cerebral blood flow (CBF), preservation of cerebral tissue, and reduction of neurologic functional deficits (Borlongan *et al*, 2004; Li *et al*, 2011; Mahmood *et al*, 2003). In addition, grafted cells amplify endogenous regenerative and restorative processes, e.g., angiogenesis and neurogenesis (Chopp and Li, 2006; Xiong *et al*, 2010). However, there is a paucity of knowledge of whether the cell engraftment alters the dynamic profile of angiogenesis and cerebral tissue perfusion of the trauma-injured brain and subsequently impacts functional outcome, although histological evaluation reveals that TBI induces angiogenesis (Morgan *et al*, 2007) and cell transplantation after TBI augments this endogenous event (Qu *et al*, 2008; Xiong *et al*, 2009*b*). The majority of

Correspondence: Dr Q Jiang, Department of Neurology, Henry Ford Hospital, B126, Education and Research Building, 2799 West Grand Boulevard, Detroit, MI 48202, USA.
E-mail: qjiang1@hfhs.org
This work was supported by National Institute of Neurological Disorders and Stroke grants, P50 NS23393, RO1 NS064134, RO1 NS48349, RO1 NS43324, HL64766, and the Mort and Brigitte Harris Foundation.
Received 21 November 2011; revised 4 June 2012; accepted 26 June 2012; published online 11 July 2012

studies on cell-based treatment have been performed with cells injected at 1 or more days after TBI (Mahmood *et al*, 2003; Xiong *et al*, 2009*b*). And there are few studies on the dynamic response of a traumatized brain to an early cell intervention, i.e., within 24 hours. Acute treatment of TBI is clinically feasible and could facilitate functional recovery through both neuroprotective and neurorestorative action (Iihoshi *et al*, 2004).

Magnetic resonance imaging (MRI) can longitudinally monitor the hemodynamic, morphological, and structural status of the living brain (Cunningham *et al*, 2005; Kochanek *et al*, 2002; Li *et al*, 2009). Also, MRI can visualize angiogenesis after brain insult (Chopp *et al*, 2007; Jiang *et al*, 2005; Seevinck *et al*, 2010). Using a widely used animal model of TBI and a 6-week observation window, the objectives of the present study were to (1) investigate the therapeutic effect of early intravenous administration (6 hours after injury) of human marrow stromal cells (hMSCs) on the trauma-injured brain, and (2) test the hypothesis that transplantation of hMSCs after TBI promotes postinjury brain angiogenesis, which can be dynamically revealed by *in-vivo* MRI and may contribute to the improved functional recovery.

Materials and methods

All experimental procedures were conducted in accordance with the NIH Guide for the Care and Use of Laboratory Animals and approved by the Institutional Animal Care and Use Committee of Henry Ford Health System.

Animal Model and Cell Transplantation Procedures

Under aseptic conditions, male Wistar rats (300 to 350 g, $n = 18$) were intraperitoneally anesthetized with chloral hydrate (350 mg/kg body weight) and their rectal temperature was maintained at 37°C with a feedback-regulated water-heating pad. The head of each animal was mounted in a stereotactic frame and two 10-mm-diameter craniotomies were performed adjacent to the central suture, midway between the lambda and the bregma, leaving the dura mater over the cortex intact. The left craniotomy confined the location of experimental impact while the right one allowed for the lateral movement of cortical tissue. Using a controlled cortical impact device, TBI was induced by delivering a single impact at a velocity of 4 m/s and a depth of 2.5 mm to the left cortex with a pneumatic piston containing a 6-mm-diameter tip (Mahmood *et al*, 2004). After the operation, the bone flap was replaced and sealed with bone wax, and the skin was sutured. For analgesia, Buprenex (0.05 mg/kg, subcutaneously) was administered to each animal after brain injury. This animal model produces a severe TBI with contusion lesion affecting part of the primary motor, secondary motor, and primary somatosensory cortex.

The hMSCs were provided by Theradigm (Baltimore, MD, USA). Before injection into rats, the cells were suspended in phosphate-buffered saline. To investigate the effect of acute cell intervention on brain remodeling, cell transplantation was conducted 6 hours after TBI. Rats subjected to TBI were randomized to one of the two treatment groups, cell- and saline-treated groups. Anesthesia was reinstituted before the transplantation and a bolus of the cell suspension ($\sim 3 \times 10^6$ hMSCs in 1 mL phosphate-buffered saline) was slowly infused over a 5-minute period into the tail vein of each rat in the cell-treated group ($n = 9$) using a Hamilton syringe. The needle was left in place for 1 minute before withdrawal to minimize cell leakage and the injection site was compressed for a short time to reduce bleeding. Replacing the cell suspension with the same amount of saline, each animal in the saline-treated group ($n = 9$) underwent the identical procedure as those in the cell-treated group. No immunosuppressants were used in this study since MSCs are hypoimmunogenic (Rossignol *et al*, 2009).

In-vivo Magnetic Resonance Imaging

Magnetic Resonance imaging was performed using a 7-Tesla, 20-cm bore superconducting magnet (Magnex Scientific, Abingdon, UK) interfaced to a Bruker console (Bruker BioSpin, Billerica, MA, USA). The animal was securely fixed on a nonmagnetic holder equipped with a nose cone for administration of anesthetic gases and stereotaxic ear bars to limit motion of the head. A tri-pilot scan of imaging sequence was used for reproducible positioning of the animal in the magnet at each MRI session. During image acquisition, anesthesia was maintained by mechanically ventilating with 1.0% halothane in 69% N_2O and 30% O_2, and rectal temperature was kept at 37 ± 1.0°C using a feedback-controlled water bath underneath the animal. T2-weighted imaging, CBF, three-dimensional (3D) gradient echo imaging and blood-to-brain transfer constant (Ki) of gadolinium-diethylenetriamine pentaacetic acid were acquired for all animals 2 days after TBI, and then weekly for 6 weeks. All rats were killed after the final *in-vivo* MRI scans.

T2-weighted imaging was acquired using a standard two-dimensional multislice (13 slices, 1 mm thick), multiecho (6 echoes) sequence. Six sets of images (13 slices per set) were obtained using echo times of 15, 30, 45, 60, 75, and 90 ms and a repetition time of 8 seconds. Images were obtained using a $32 \times 32\,mm^2$ field of view and a 128×64 image matrix.

The continuous arterial spin labeling technique was used to quantify CBF in cerebral tissue. The adiabatic inversion of arterial water protons was accomplished *via* an axial gradient of 0.3 kHz/mm and a 1-second continuous radio frequency power wave of ~ 0.3 kHz at a frequency offset of 6 kHz. This was followed by a spin echo imaging sequence with repetition time/echo time = 1,000/20 ms. The labeled slice was positioned ± 2 cm from the imaging slice, which was 1 mm thick. To eliminate gradient asymmetry in the axial direction, an image average was applied by switching around the gradient polarities. Field of view was $32 \times 32\,mm^2$ and the image matrix was 64×64.

The 3D gradient echo images were acquired with repetition time of 40 ms, echo time of 10 ms, flip angle of 15°,

and a $32 \times 32 \times 24\,mm^3$ field of view. The $256 \times 192 \times 64$ image matrix was interpolated to $256 \times 256 \times 64$ for analysis.

To measure the Ki, a Look-Locker sequence was used to acquire dynamic T_1 maps (Ewing *et al*, 2003). After one set of baseline T_1 maps was collected (five interleaved slices), a bolus of 0.2 mmol/kg gadolinium-diethylenetriamine pentaacetic acid was manually injected in less than 5 seconds after a 0.4 mL saline flush via tail vein. Then, ten sets of T_1 maps were acquired sequentially at ~2.5-minute intervals for the next 25 minutes ($32 \times 32\,mm^2$ field of view, 128×64 matrix, 2 mm slice thickness). Under the assumption that a change in $1/T_1$ ($\Delta R_1(t)$) is linearly proportional to a change in both plasma ($C_{pa}(t)$) and tissue ($C_{tis}(t)$) concentrations of contrast agent and the assumption that the constant of proportionality is the same for tissue and blood, $\Delta R_1(t)$s measured in tissue ($\Delta R_{1tis}(t)$) and sagittal sinus ($\Delta R_{1pa}(t)$) were used as estimates of $C_{tis}(t)$ and $C_{pa}(t)$, respectively. Using Patlak plots (Ewing *et al*, 2003), linear least-squares estimates of slope (Ki) were determined for each pixel and maps of Ki were constructed.

Magnetic Resonance Imaging Data Processing

The lateral ventricle and the cortical lesion are easily visualized on the T2 map as marked hyperintensities and the border between them could entirely disappear, particularly at the later stage of TBI, due to the expansion of both areas. To accurately measure these two distinct regions, we use the T2 map to identify the hyperintensity encompassing both the ipsilateral ventricle and cortical lesion, and structural information revealed by 3D image to distinguish cortical lesion from the ipsilateral ventricle, as previously reported (Li *et al*, 2011).

The ventricle and lesion areas on the T2 maps are specified by hyperintense pixels with a T2 value higher than the mean plus twice the standard deviation (mean + 2s.d.) provided by the normal tissue on the contralateral (noninjured) side (Li *et al*, 2011). The trauma-induced lesion in each slice was identified using the above criteria, and the lesion volume was then calculated on the basis of lesion areas on individual slices and slice thickness. The lateral ventricle was measured at a fixed structural location presented by four contiguous coronal T2 slices (approximately at level of bregma −2.8 to bregma 1.2) for all animals (Li *et al*, 2011). Similarly, the ventricular volume was obtained by adding all the areas measured on individual slices and multiplying the total by the slice thickness. Data are presented as ventricle volumes in the ipsilateral and contralateral sides of the brain.

Hyperpermeability was identified on the Ki map as significantly elevated regions against roughly consistent background (mean + 2s.d.) where no leakage occurs. These regions on Ki maps were monitored for their location and time point of first appearance.

To quantify TBI-induced hypoperfusion, a viability threshold for CBF (30 mL/100 g per minute) derived from experimental ischemia (Shen *et al*, 2004) was used to detect the location and extent of tissue regions with perfusion abnormality. Areas with CBF lower than this threshold were identified on the CBF map (ventricles were excluded) and presented as percentage of the examined slice.

Measurements were performed for each animal in both cell- ($n = 9$) and saline-treated ($n = 9$) groups and the data were averaged at the same time points for each group.

Modified Neurologic Severity Score

The modified neurologic severity score (mNSS; Xiong *et al*, 2009*b*) grades the composite neurologic function of an animal on motor, sensory, reflex, and balance tests. One point is awarded for the inability of an animal to perform the tasks correctly or for the lack of a tested reflex (normal score: 0; maximal deficit score: 18). Therefore, the higher score indicates the more severe neurologic dysfunction. The mNSS was assessed for each animal preTBI and postTBI on days 1, 4, and weekly thereafter by an examiner blinded to the treatment groups and the corresponding MRI results.

Modified Morris Water Maze Test

To evaluate the long-term functional outcome of spatial learning acquisition and memory retention, the modified Morris water maze test (Li *et al*, 2011) was used. The testing system consisted of a circular tank (140 cm in diameter and 45 cm high) filled with 30°C water and a hidden platform (15 cm in diameter and 35 cm high) set inside the tank 1.5 cm below the surface of the water. The pool was located in a large test room decorated with visual clues (for example, pictures and lamps) that remained constant during the study and enabled the rats to orientate themselves spatially. For descriptive data collection, an automated tracking system (HVS Image, San Diego, CA, USA) was used and the pool was subdivided into four equal quadrants formed by imaging lines.

The rats were tested on 5 consecutive days (1 trial per day) at the later stage of TBI (from day 31 to 35 after TBI). Each trial was initiated by placing the animal randomly at one of the four start locations (North, South, East, and West) and allowing 90 seconds to find the hidden platform. The platform was put in a randomly changing position within the Northeast quadrant throughout the test period (e.g., sometimes equidistant from the center and edge of the pool, against the wall, near the center of the pool, and at the edges of the Northeast quadrant). Upon locating the platform, the animal was allowed to remain on the platform for 15 seconds before being returned to its cage. If the animal failed to find the platform within 90 seconds, then the experiment was terminated and a maximum score of 90 seconds was assigned. The percentage of time traveled within the Northeast (correct) quadrant was calculated relative to the total amount of time spent swimming before reaching the platform.

Tissue Preparation and Histology

Immediately after the final *in-vivo* MRI measurements at 6 weeks after TBI, rats were deeply anesthetized with

ketamine and xylazine, and transcardially perfused with heparinized saline, followed by 4% paraformaldehyde (Li *et al*, 2011). The brains were removed shortly after death and placed in 4% paraformaldehyde in phosphate-buffered saline at 4°C for 2 days, and then cut into seven standard coronal blocks 2 mm thick on a rodent brain matrix. Coronal sections of 6 μm thick were sliced from each block, embedded in paraffin and stained for histological evaluation.

For morphological analysis and quantification of cerebral vessels, endothelial barrier antigen (EBA) immunohistological staining was used. Sections were deparaffinized, hydrated, and antigen retrieved with citrate buffer (pH 6.0, 10 minutes), then treated with 3% hydrogen peroxide to quench nonspecific peroxidase staining, followed by 1% bovine serum albumin in phosphate-buffered saline to block nonspecific protein binding. Sections were incubated with a monoclonal antibody to EBA at a dilution of 1:1,000 for 18 hours at 4°C (Covance SMI-71, Berkeley, CA, USA). Negative controls were performed by incubating the sections with species-specific normal serum. The sections were incubated in biotinylated goat anti-mouse IgM (Vector, Burlingame, CA, USA) at a dilution of 1:200 for 30 minutes followed by avidin-biotin-peroxidase complex for 30 minutes at room temperature (Vector # PK-6100) and then visualized with 3,3′-Diaminobenzidine (Sigma-Aldrich, St Louis, MO, USA). Sections were counterstained with Mayer's hematoxylin (Rowley Biochem., Danvers, MA, USA). The EBA-immunostained tissue sections were digitized using a 3-CCD color video camera (Sony DXC-970MD; Ampronix Inc., Irvine, CA, USA) interfaced with MCID image analysis system (Imaging Research Inc., St Catherines, ON, Canada). Numbers of vessels were counted in four regions surrounding the lesion (DG, CA1, CA3, and peri-contusional cortex) on a fixed reference coronal section (approximately at level of bregma −2.8) for all animals, which contained the TBI-induced lesion and matched the MRI slice. In each region, three nonoverlapping fields of the same size view were digitized under a $\times 40$ objective. Measurements were performed in both the ipsilateral and contralateral sides in the same regions and data are presented as the average vessel number per square millimeter.

Statistical Analysis

Statistical analysis was performed using SAS (Cary, NC, USA, version 9.2). Analysis of covariance was used to compare the group difference in MRI measurements (hypoperfusion area, lesion, and ventricle volumes) and functional assessments (mNSS and water maze test) with the independent factor of treatment and dependent factor of time. The treatment effect on mNSS was conducted based on the ranked data, since the data were not normally distributed. Analysis began with testing the treatment group and time interaction, followed by testing the group difference at each time point and the time effect for each treatment group if the interaction or the overall group/time effect was detected at the 0.05 level. A subgroup analysis would be considered if the interaction or main effect of group/time was not at the 0.05 level. Kaplan–Meier approach was performed to test the group difference in time point for angiogenesis being detected in the injured brain, using the log-rank test with the estimated median time (the time at which angiogenesis was detected in 50% of subjects studied). Using Analysis of Variance, the association between earlier onset of angiogenesis (present at 3 weeks or earlier) and MRI, histological and functional measurements was studied. Vessel density for each specific brain region was analyzed by two-sample *t*-test. Results are presented as mean ± standard error (s.e.). Statistical significance was inferred for $P \leq 0.05$.

Results

Lesion and Ventricular Volume Changes Measured from T2 Map

The temporal profiles of lesion and ventricular volumes for the two treatment groups are given in Figure 1. Although no significant group difference in lesion volume was detected over a 6-week observation period, the mean values of lesion volume in the cell-treated group were lower than in the saline-treated group (Figure 1A). Compared with the saline-treated group, treatment with hMSCs significantly reduced ventricular dilation (Figures 1B and 1C, 1 to 6 weeks, $P < 0.05$) in both the ipsilateral (Figure 1B) and contralateral sides (Figure 1C) of the brain, suggesting that hMSCs reduce cerebral atrophy.

Hyperpermeability

As shown in Figure 2, hyperpermeabilities on the Ki map in the injured brain (red arrows in Figures 2A and 2B), indicative of the vascular leakage, appeared at acute (Figure 2A) and at later (Figure 2B) time points after TBI. While the elevated area on the Ki map at the acute time usually presents at or near the location of primary impact (comparing Figure 2A with 2C) and indicates breakdown of the BBB (Li *et al*, 2011), the elevation of Ki area at later times is apparent adjacent to the lesion boundary (comparing Figure 2B with 2D) and is indicative of angiogenesis (Jiang *et al*, 2005). Our dynamic measurements showed that increased permeability indicative of BBB damage was detected soon after injury, and in some cases persisted up to 1 week after TBI. The leakage induced by angiogenesis (newly formed blood vessels with immature BBB) was observed from 2 to 6 weeks after TBI. Using the elevated area on the Ki map, indicative of BBB damage or angiogenesis, as an ROI (region of interest) and calculating the mean value relative to that in the contralateral homologous tissue area (relative Ki), the representative Ki profiles for these two distinct regions are presented in Figure 2E. Each animal may exhibit a unique temporal pattern, especially for the angiogenesis region, since the initiation of angiogenesis varies with animals after TBI even in

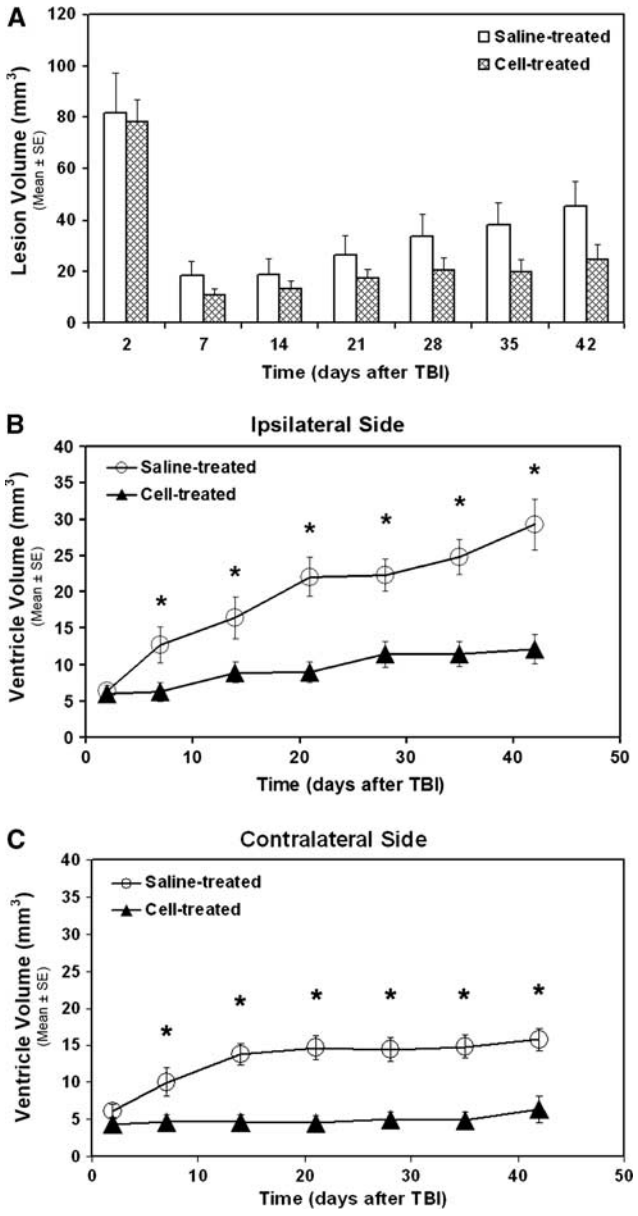

Figure 1 Volumetric changes in cortical lesion (**A**) and lateral ventricles (**B**, **C**) identified on T2 map. No significant group difference in T2 lesion volume was found over a 6-week observation period (**A**). Cell administration after traumatic brain injury (TBI) significantly reduced ventricular expansion in both the ipsilateral (**B**, 1 to 6 weeks, $*P < 0.05$) and contralateral sides (**C**, 1 to 6 weeks, $*P < 0.05$) of the brain.

the same treatment group. Our observation indicated that angiogenic area identified on the Ki map became apparent 2 to 3 weeks and 3 to 4 weeks after TBI in the cell- and saline-treated groups, respectively. Statistical analysis showed that Ki-detected angiogenesis occurred significantly earlier in the cell-treated group than in the saline-treated group (Figure 2F, estimated median time: 2 versus 4 weeks after injury, $P < 0.05$).

The angiogenic area identified on the Ki map (Figure 2B) was confirmed histologically by the presence of enlarged thin-walled vessels (Figure 2G), which differed morphologically from the vessels (Figure 2H) seen in the homologous tissue area in the contralateral side of the brain. Quantitative data revealed a significantly higher vessel density in the lesion boundary region in the cell-treated group than in the saline-treatment group (Figure 2I).

Hypoperfusion

The temporal profiles of hypoperfusion status for both treatment groups are shown in Figure 2J. Along with time after brain injury, the area with lower CBF in the cell-treated group gradually decreased, while this tendency was less evident in the saline-treated group during the same observation period. A significant group difference was detected at 3, 4, 5, and 6 weeks after TBI.

Outcome of Neurologic Function

A reduced functional impairment was detected in the cell-treated group as compared with the saline-treated group (Figure 3). Neurologic severity score (mNSS) awarded to the saline-treated animals was significantly higher than to the cell-treated animals (Figure 3A, 2 to 5 weeks, $P < 0.05$). The cell-treated animals spent significantly longer times in the correct quadrant than the saline-treated animals (Figure 3B, 33 to 35 days, $P < 0.05$).

Association Analysis

To investigate the effect of angiogenesis on histological and functional outcome, association analysis was performed. Angiogenesis that presented on the Ki map at 3 weeks or earlier was considered as an early onset angiogenesis. Animals were divided into earlier and later angiogenesis groups, and the mean values in vessel density and behavior grade between the groups were compared using Analysis of Variance test. As shown in Figure 4, earlier angiogenesis was significantly associated with higher vessel density seen in the cortex boundary region (Figure 4A, $P < 0.05$) and was marginally associated with improved behavioral status (modified Morris Water Maze Test) assessed at 35 days (Figure 4B, $P < 0.06$), suggesting that early onset of angiogenesis contributes to the histological and functional recovery.

Discussion

Using MRI, trauma-induced morphological and hemodynamic abnormalities in the injured brain and the temporal profile of angiogenesis after the injury with or without cell intervention were longitudinally investigated *in vivo*. Our data showed that treatment of TBI with intravenous administration of hMSCs at 6 hours after brain trauma, an acute time

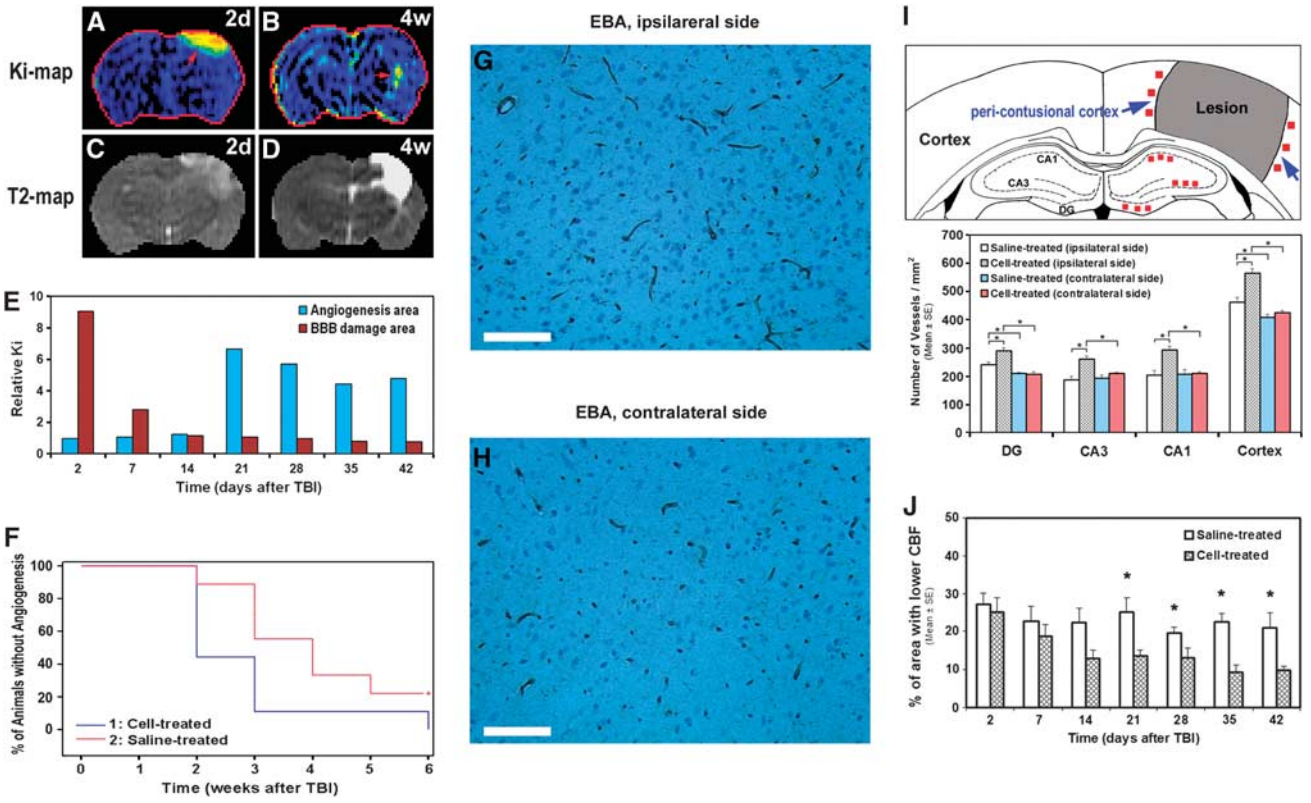

Figure 2 Hyperpermeabilities (**A** and **B**, red arrows), T2 lesion (**C** and **D**, hyperintensities), Ki profile (**E**), statistical result (**F**), blood vessels revealed by endothelial barrier antigen (EBA)-immunostained tissue section (**G**, **H**), schematic diagram of microscopic regions and vessel density (**I**), and evolution of hypoperfusion (**J**). Elevated area on Ki map at acute time usually presents at or near the location of primary impact (comparing **A** with **C**) and indicates blood–brain barrier (BBB) breakdown. This hyperpermeability at a later stage is apparent nearby the lesion (comparing **B** with **D**) and is suggestive of angiogenesis. The representative Ki profile obtained from a saline-treated animal for these two distinct regions (**E**) shows: (1) the BBB breakdown area with the elevated Ki lasting for 1 week; and (2) the angiogenesis area with hyperpermeability on the Ki map starting at 3 weeks after injury and persisting thereafter for several weeks. A higher percentage of animals without angiogenesis was detected in the saline-treated group than in the cell-treated group during 2 to 6 weeks (**F**). Analysis showed that Ki-detected angiogenesis occurred significantly earlier in the cell-treated group than in the saline-treated group (estimated median time: 2 versus 4 weeks after injury, $P < 0.05$). Angiogenic area present on the Ki map (**B**, red arrow) was confirmed by enlarged thin-walled vessels (**G**) on EBA-stained tissue slice as compared with the vessels (**H**) in the homogeneous tissue area in the contralateral side of the brain (scale bar in **G** and **H** = 100 μm). Histological analysis (6 weeks after TBI) revealed a significantly higher vessel density in the lesion boundary region in the cell-treated group than in the saline-treatment group (**I**, $^*P < 0.05$). Cell transplantation after TBI led to apparent amelioration of hypoperfusion state (**J**) and significant group difference in hypoperfusion area was detected between the treatment groups (3 to 6 weeks, $^*P < 0.05$). TBI, traumatic brain injury.

point, preserved cerebral tissue, limited the extent of hypoperfusion and reduced neurologic deficits. We showed that administration of hMSCs led to an early presence and amplified angiogenesis in the trauma-injured brain, which may contribute to the amelioration of the hypoperfusion state and the improvement of functional outcome at the late stage of TBI.

To date, there is no clinical treatment available for TBI patients to effectively prevent secondary injury and promote functional recovery (Parr *et al*, 2007). Cumulative data indicate that cell transplantation, which stimulates endogenous restorative processes, provides promising therapeutic strategies for reversing neurologic deficits after central nervous system injury, including TBI (Chopp and Li, 2006). One of the postinjury restorative processes activated by cell-based therapies, which promotes functional improvement, is angiogenesis (Chen *et al*, 2003; Jiang *et al*, 2005; Xiong *et al*, 2009*b*; Zacharek *et al*, 2007), a repair process whereby new blood vessels develop from preexisting ones in response to tissue metabolic demands (Plate, 1999). This newly formed vascular network, which may reestablish a functional microvasculature in the lesion boundary region, paves the way for possible repair of the injured cerebral tissue. The expanded vasculature also increases the production and release of trophic factors, like brain-derived neurotrophic factor and others, contributing to functional recovery (Chen *et al*, 2005; Leventhal *et al*, 1999). As a transient biological process, the temporal evolution of cerebral angiogenesis may influence the restoration of blood

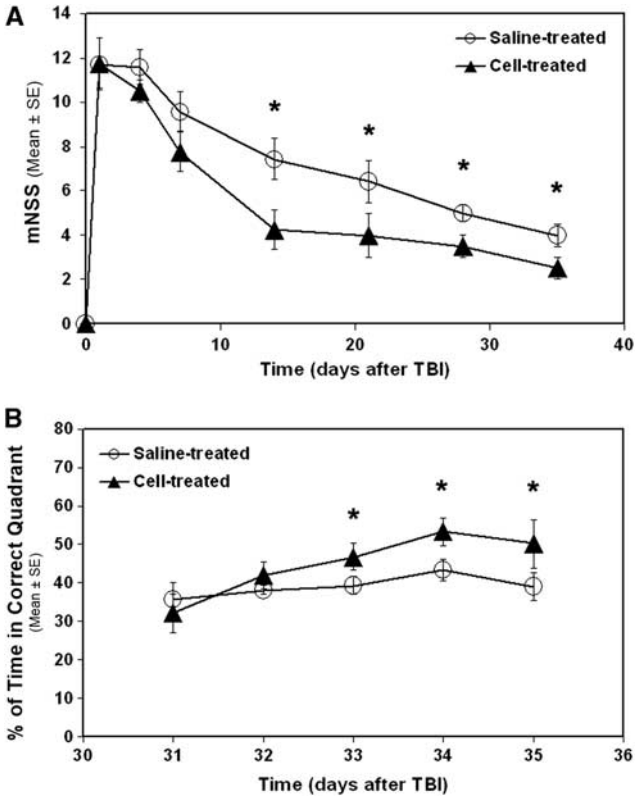

Figure 3 Line graphs illustrating functional outcome after traumatic brain injury (TBI). Significantly higher modified neurologic severity score (mNSS) numbers were awarded to the saline-treated animals than to the cell-treated animals (**A**, 2 to 5 weeks, $*P < 0.05$). The cell-treated animals spent significantly longer time in the correct quadrant than the saline-treated animals (**B**, 33 to 35 days, $*P < 0.05$).

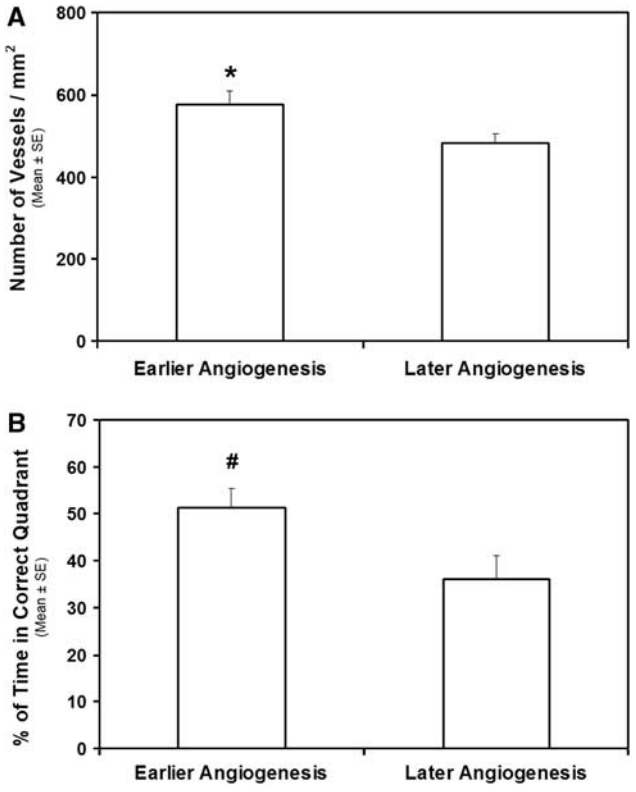

Figure 4 Results of association analysis. Earlier angiogenesis was significantly associated with higher vessel density seen in the cortex boundary region (**A**, $*P < 0.05$) and was marginally associated with improved behavioral status (modified Morris Water Maze Test, mWMT) assessed at 35 days (**B**, $^{\#}P < 0.06$).

supply and, in turn, determine the fate of hypoperfusion-affected neuronal tissue. The earlier the event occurs, the more likely the tissue is rescued from ischemic damage. In the previous investigations, however, less attention was paid to the dynamic pattern of this reparative process, particularly in the traumatized brain, as compared with the considerable effort devoted to the angiogenic intensity and the corresponding spatial features measured by means of histopathology (Morgan *et al*, 2007; Wu *et al*, 2011; Xiong *et al*, 2009*b*).

Magnetic resonance imaging can noninvasively detect angiogenesis *in vivo* by visualizing vascular hyperpermeability (Chopp *et al*, 2007; Jiang *et al*, 2005; Seevinck *et al*, 2010), indicated by the leakage of tracer (contrast agent) from the newly generated blood vessels with immature BBB (Pettersson *et al*, 2000). Although increased permeability shown on the Ki map could be caused by BBB disruption or angiogenesis, their different temporal sequence and localization readily distinguish one from the other. While elevated areas on the Ki map that represent BBB breakdown occur at or near the site of primary impact soon after TBI, angiogenesis-induced hyperintensities appear adjacent to the lesion from 2 to 6 weeks after TBI. The angiogenic area identified on the Ki map was confirmed by enlarged thin-walled vessels (Figure 2G), the histological evidence of angiogenesis, present in the corresponding tissue region. Consistent with a previous report (Xiong *et al*, 2009*b*), the increased number of these vessels in proximity to the lesion appeared after cell transplantation (Figure 2I), indicative of an enhanced angiogenesis. Our longitudinal measurements showed that cell engraftment significantly altered the temporal profile of angiogenesis and induced an earlier development of this endogenous process in the cell-treated animals compared with the saline-treated animals (Figure 2F, 2 versus 4 weeks for the cell- and saline-treated groups, respectively). Importantly, earlier onset of angiogenesis (present at 3 weeks or earlier) was highly associated with a higher vessel density in the boundary region (Figure 4A) and an improved neurologic performance assessed at a late stage of TBI (Figure 4B). These results indicate that cell treatment after TBI induces early angiogenesis, which exerts beneficial effects on histological and functional recovery.

As a potential mechanism involved in the induction of secondary injury, TBI-induced hypoperfusion widely affects the injured brain. In addition to the

area of primary impact, hypoperfusion heterogeneously occurs in regions remote from the site of impact, even in the hemisphere contralateral to the injury (Bonne *et al*, 2003; Pasco *et al*, 2007). To quantify the state of this hemodynamic abnormality, a threshold for CBF (30 mL/100 g per minute), which is much lower than the normal level of CBF in the rat brain ($\sim$140 mL/100 g per minute) (Shen *et al*, 2004), was used to identify the extent of hypoperfusion. Our dynamic data showed that cell administration led to a gradually restored perfusion as indicated by the reduced hypoperfusion area with time after TBI (Figure 2J). The change of hypoperfusion area, however, was not apparent for the saline-treated animals during the same observation period. The earlier onset of angiogenesis induced by cell administration (Figure 2F), which occurs concomitantly with an increased density of blood vessels (Figure 2I), is a crucial factor for the accelerated restoration of perfusion, although the effect of MSCs on BBB reconstitution and vascular stabilization (Borlongan *et al*, 2004; Zacharek *et al*, 2007) also contributes to the beneficial results. The restored perfusion may counteract oxygen and nutrition deficiency, thus reducing ongoing cell death, promoting neural plasticity in a neuroprotective microenvironment which subsequently improves brain function. Our dynamic observations support this hypothesis and show that earlier onset of angiogenesis (Figure 2F, 2 versus 4 weeks for the cell- and saline-treated groups, respectively) leads to lower hypoperfusion area in the injured brain and improved functional performance (comparing Figure 2J with Figure 3A).

Upon transplantation, MSCs responsively secrete and stimulate within the parenchymal tissue an array of growth and trophic factors adjusted to the needs of the compromised tissue (Chen *et al*, 2002; Chopp and Li, 2006; Mahmood *et al*, 2004), including brain-derived neurotrophic factor, vascular endothelial growth factor, basic fibroblast growth factor, hepatocyte growth factor, and nerve growth factor. Attempting to protect the brain against the physiological and biochemical cascades triggered by the traumatic insult, these factors act on different target cells and serve different functions in the postinjury brain. Early development of angiogenesis observed in the cell-treated animals may be attributed to the elevated level of vascular endothelial growth factor and basic fibroblast growth factor, potent angiogenic agents, in the injured brain. These stimulatory factors are expressed before the onset of neovascularization (Chen *et al*, 1994; Nag *et al*, 1997; Plate, 1999). As shown previously, the majority of administered cells preferentially home to the injured hemisphere surrounding the lesion (Li *et al*, 2011; Mahmood *et al*, 2004) where growth factors are significantly upregulated in response to cell engraftment (Mahmood *et al*, 2004; Qu *et al*, 2011) and angiogenesis occurs (Xiong *et al*, 2009*b*). Also, the transplanted cells arrive at the cerebral destination followed by the appearance of angiogenesis, as previously reported (Li *et al*, 2006, 2010). The temporal and spatial coincidence between grafts, growth factors, and angiogenesis support our hypothesis that engrafted cells, particularly by their secretion and/or induction of specific factors essential for angiogenic process (Plate, 1999), promote the development of angiogenesis in the host brain. Except for enhanced angiogenesis (Figure 2I) and restored perfusion (Figure 2J) after cell transplantation, the reduced cerebral atrophy (Figures 1B and 1C) and improved functional outcome (Figure 3) may derive in part from the ability of these factors to provide survival-supporting and protective effects on neurons, and antiapoptotic actions (Chopp and Li, 2006; Shen *et al*, 2010; Thau-Zuchman *et al*, 2010) which lessen the degree of degeneration after TBI.

Our data confirm previous findings (Li *et al*, 2011; Qu *et al*, 2008) that treatment of TBI with intravenous transplantation of hMSCs preserves the cerebral tissue (Figures 1B and 1C), ameliorates the hypoperfusion status (Figure 2J), and improves functional recovery (Figures 3A and 3B). These therapeutic effects can be achieved either after acute injection, as conducted in the present study, or after delayed administration (Li *et al*, 2011), indicating a wide intravenous intervention window for MSCs therapy. However, the significant therapeutic effects of hMSC treatment on reduction of ventricular expansion and decrease of mNSS were present at earlier time points after acute transplantation (1 to 2 weeks) than after delayed engraftment (2 to 3weeks). These data suggest that acute cell intervention extends the time range of therapeutic benefit by initiating the therapeutic effects earlier and that the earlier the cell transplantation is performed after TBI the greater the beneficial outcome. As shown in Figures 1B and 1C, the therapeutic effects resulting from acute cell administration occur as early as 1 week after TBI. This period of time after TBI may be too early to be primarily mediated by the induction of restorative processes, as shown by our current data. Instead, the outcome may derive from the contribution of neurotrophins that are rapidly produced in the host brain within this time (Chen *et al*, 2002; Mahmood *et al*, 2004). Meanwhile, significantly reduced apoptosis (Shen *et al*, 2010) in the injured brain may also account for attenuated impairment. Therefore, the cell-induced benefit detected at the early stage of TBI, such as 1 week after TBI, may be primarily attributed to neuroprotective as well as antiapoptotic effects of MSCs rather than their neurorestorative action. Recruiting both protective and restorative function of MSCs may result in an advanced therapeutic effect seen after acute cell administration.

In summary, intravenous transplantation of hMSCs at 6 hours after TBI, an acute time point, leads to less cerebral atrophy, lower hypoperfusion area, and better functional status as compared with controls. The engraftment evokes an enhanced angiogenesis in the injured brain, which occurs early and likely has

an important role in expeditious restoration of disturbed perfusion and improvement of functional outcome at the late stage of TBI.

Disclosure/conflict of interest

The authors declare no conflict of interest.

References

Bonne O, Gilboa A, Louzoun Y, Kempf-Sherf O, Katz M, Fishman Y, Ben-Nahum Z, Krausz Y, Bocher M, Lester H, Chisin R, Lerer B (2003) Cerebral blood flow in chronic symptomatic mild traumatic brain injury. *Psychiatry Res* 124:141–52

Borlongan CV, Lind JG, Dillon-Carter O, Yu G, Hadman M, Cheng C, Carroll J, Hess DC (2004) Intracerebral xenografts of mouse bone marrow cells in adult rats facilitate restoration of cerebral blood flow and blood-brain barrier. *Brain Res* 1009:26–33

Chen HH, Chien CH, Liu HM (1994) Correlation between angiogenesis and basic fibroblast growth factor expression in experimental brain infarct. *Stroke* 25:1651–7

Chen J, Zhang C, Jiang H, Li Y, Zhang L, Robin A, Katakowski M, Lu M, Chopp M (2005) Atorvastatin induction of VEGF and BDNF promotes brain plasticity after stroke in mice. *J Cereb Blood Flow Metab* 25: 281–90

Chen J, Zhang ZG, Li Y, Wang L, Xu YX, Gautam SC, Lu M, Zhu Z, Chopp M (2003) Intravenous administration of human bone marrow stromal cells induces angiogenesis in the ischemic boundary zone after stroke in rats. *Circ Res* 92:692–9

Chen X, Katakowski M, Li Y, Lu D, Wang L, Zhang L, Chen J, Xu Y, Gautam S, Mahmood A, Chopp M (2002) Human bone marrow stromal cell cultures conditioned by traumatic brain tissue extracts: growth factor production. *J Neurosci Res* 69:687–91

Chopp M, Li Y (2006) Transplantation of bone marrow stromal cells for treatment of central nervous system diseases. *Adv Exp Med Biol* 585:49–64

Chopp M, Zhang ZG, Jiang Q (2007) Neurogenesis, angiogenesis, and MRI indices of functional recovery from stroke. *Stroke* 38:827–31

Cunningham AS, Salvador R, Coles JP, Chatfield DA, Bradley PG, Johnston AJ, Steiner LA, Fryer TD, Aigbirhio FI, Smielewski P, Williams GB, Carpenter TA, Gillard JH, Pickard JD, Menon DK (2005) Physiological thresholds for irreversible tissue damage in contusional regions following traumatic brain injury. *Brain* 128:1931–42

Ewing JR, Knight RA, Nagaraja TN, Yee JS, Nagesh V, Whitton PA, Li L, Fenstermacher JD (2003) Patlak plots of Gd-DTPA MRI data yield blood-brain transfer constants concordant with those of 14C-sucrose in areas of blood-brain opening. *Magn Reson Med* 50:283–92

Iihoshi S, Honmou O, Houkin K, Hashi K, Kocsis JD (2004) A therapeutic window for intravenous administration of autologous bone marrow after cerebral ischemia in adult rats. *Brain Res* 1007:1–9

Jiang Q, Zhang ZG, Ding GL, Zhang L, Ewing JR, Wang L, Zhang R, Li L, Lu M, Meng H, Arbab AS, Hu J, Li QJ, Pourabdollah Nejad DS, Athiraman H, Chopp M (2005) Investigation of neural progenitor cell induced angiogenesis after embolic stroke in rat using MRI. *Neuroimage* 28:698–707

Kochanek PM, Hendrich KS, Dixon CE, Schiding JK, Williams DS, Ho C (2002) Cerebral blood flow at one year after controlled cortical impact in rats: assessment by magnetic resonance imaging. *J Neurotrauma* 19:1029–37

Leventhal C, Rafii S, Rafii D, Shahar A, Goldman SA (1999) Endothelial trophic support of neuronal production and recruitment from the adult mammalian subependyma. *Mol Cell Neurosci* 13:450–64

Li L, Jiang Q, Ding G, Zhang L, Zhang ZG, Li Q, Panda S, Kapke A, Lu M, Ewing JR, Chopp M (2009) MRI identification of white matter reorganization enhanced by erythropoietin treatment in a rat model of focal ischemia. *Stroke* 40:936–41

Li L, Jiang Q, Ding G, Zhang L, Zhang ZG, Li Q, Panda S, Lu M, Ewing JR, Chopp M (2010) Effects of administration route on migration and distribution of neural progenitor cells transplanted into rats with focal cerebral ischemia, an MRI study. *J Cereb Blood Flow Metab* 30:653–62

Li L, Jiang Q, Qu CS, Ding GL, Li QJ, Wang SY, Lee JH, Lu M, Mahmood A, Chopp M (2011) Transplantation of marrow stromal cells restores cerebral blood flow and reduces cerebral atrophy in rats with traumatic brain injury: *in vivo* MRI study. *J Neurotrauma* 28:535–45

Li L, Jiang Q, Zhang L, Ding G, Wang L, Zhang R, Zhang ZG, Li Q, Ewing JR, Kapke A, Lu M, Chopp M (2006) Ischemic cerebral tissue response to subventricular zone cell transplantation measured by iterative self-organizing data analysis technique algorithm. *J Cereb Blood Flow Metab* 26:1366–77

Mahmood A, Lu D, Chopp M (2004) Intravenous administration of marrow stromal cells (MSCs) increases the expression of growth factors in rat brain after traumatic brain injury. *J Neurotrauma* 21:33–9

Mahmood A, Lu D, Lu M, Chopp M (2003) Treatment of traumatic brain injury in adult rats with intravenous administration of human bone marrow stromal cells. *Neurosurgery* 53:697–702; discussion 702-693

Masel BE, DeWitt DS (2010) Traumatic brain injury: a disease process, not an event. *J Neurotrauma* 27:1529–40

Morgan R, Kreipke CW, Roberts G, Bagchi M, Rafols JA (2007) Neovascularization following traumatic brain injury: possible evidence for both angiogenesis and vasculogenesis. *Neurol Res* 29:375–81

Nag S, Takahashi JL, Kilty DW (1997) Role of vascular endothelial growth factor in blood-brain barrier breakdown and angiogenesis in brain trauma. *J Neuropathol Exp Neurol* 56:912–21

Opydo-Chanek M (2007) Bone marrow stromal cells in traumatic brain injury (TBI) therapy: true perspective or false hope? *Acta Neurobiol Exp (Wars)* 67:187–95

Parr AM, Tator CH, Keating A (2007) Bone marrow-derived mesenchymal stromal cells for the repair of central nervous system injury. *Bone Marrow Transplant* 40: 609–19

Pasco A, Lemaire L, Franconi F, Lefur Y, Noury F, Saint-Andre JP, Benoit JP, Cozzone PJ, Le Jeune JJ (2007) Perfusional deficit and the dynamics of cerebral edemas in experimental traumatic brain injury using perfusion and diffusion-weighted magnetic resonance imaging. *J Neurotrauma* 24:1321–30

Pettersson A, Nagy JA, Brown LF, Sundberg C, Morgan E, Jungles S, Carter R, Krieger JE, Manseau EJ, Harvey VS, Eckelhoefer IA, Feng D, Dvorak AM, Mulligan RC, Dvorak HF (2000) Heterogeneity of the angiogenic

response induced in different normal adult tissues by vascular permeability factor/vascular endothelial growth factor. *Lab Invest* 80:99–115

Plate KH (1999) Mechanisms of angiogenesis in the brain. *J Neuropathol Exp Neurol* 58:313–20

Qu C, Mahmood A, Liu XS, Xiong Y, Wang L, Wu H, Li B, Zhang ZG, Kaplan DL, Chopp M (2011) The treatment of TBI with human marrow stromal cells impregnated into collagen scaffold: functional outcome and gene expression profile. *Brain Res* 1371:129–39

Qu C, Mahmood A, Lu D, Goussev A, Xiong Y, Chopp M (2008) Treatment of traumatic brain injury in mice with marrow stromal cells. *Brain Res* 1208:234–9

Rossignol J, Boyer C, Thinard R, Remy S, Dugast AS, Dubayle D, Dey ND, Boeffard F, Delecrin J, Heymann D, Vanhove B, Anegon I, Naveilhan P, Dunbar GL, Lescaudron L (2009) Mesenchymal stem cells induce a weak immune response in the rat striatum after allo or xenotransplantation. *J Cell Mol Med* 13:2547–58

Seevinck PR, Deddens LH, Dijkhuizen RM (2010) Magnetic resonance imaging of brain angiogenesis after stroke. *Angiogenesis* 13:101–11

Shen LH, Li Y, Chopp M (2010) Astrocytic endogenous glial cell derived neurotrophic factor production is enhanced by bone marrow stromal cell transplantation in the ischemic boundary zone after stroke in adult rats. *Glia* 58:1074–81

Shen Q, Ren H, Fisher M, Bouley J, Duong TQ (2004) Dynamic tracking of acute ischemic tissue fates using improved unsupervised ISODATA analysis of high-resolution quantitative perfusion and diffusion data. *J Cereb Blood Flow Metab* 24:887–97

Thau-Zuchman O, Shohami E, Alexandrovich AG, Leker RR (2010) Vascular endothelial growth factor increases neurogenesis after traumatic brain injury. *J Cereb Blood Flow Metab* 30:1008–16

Wu H, Jiang H, Lu D, Qu C, Xiong Y, Zhou D, Chopp M, Mahmood A (2011) Induction of angiogenesis and modulation of vascular endothelial growth factor receptor-2 by simvastatin after traumatic brain injury. *Neurosurgery* 68:1363–71

Xiong Y, Mahmood A, Chopp M (2009*a*) Emerging treatments for traumatic brain injury. *Expert Opin Emerg Drugs* 14:67–84

Xiong Y, Mahmood A, Chopp M (2010) Angiogenesis, neurogenesis and brain recovery of function following injury. *Curr Opin Investig Drugs* 11:298–308

Xiong Y, Qu C, Mahmood A, Liu Z, Ning R, Li Y, Kaplan DL, Schallert T, Chopp M (2009*b*) Delayed transplantation of human marrow stromal cell-seeded scaffolds increases transcallosal neural fiber length, angiogenesis, and hippocampal neuronal survival and improves functional outcome after traumatic brain injury in rats. *Brain Res* 1263:183–91

Zacharek A, Chen J, Cui X, Li A, Li Y, Roberts C, Feng Y, Gao Q, Chopp M (2007) Angiopoietin1/Tie2 and VEGF/Flk1 induced by MSC treatment amplifies angiogenesis and vascular stabilization after stroke. *J Cereb Blood Flow Metab* 27:1684–91